Focused Deposition of Electrospun Polymer Fibers

S. Neubert,[1] D. Pliszka,[1] A. Góra,[1] A. Jaworek,[2] E. Wintermantel,[3] S. Ramakrishna[1,4]

[1]*Helthcare and Energy Materials Lab, National University of Singapore, Singapore 117576*
[2]*Centre for Thermomechanics of Fluids, Institute of Fluid Flow Machinery, Polish Academy of Sciences, Fiszera 14, 80-952 Gdansk, Poland*
[3]*Department and Chair for Medical Engineering, Faculty of Mechanical Engineering, TU Muenchen (TUM), Bolzmannstr. 15, D-85748 Garching, Germany*
[4]*King Saud University, Riyadh 11451, Saudi Arabia*

Received 8 March 2011; accepted 2 September 2011
DOI 10.1002/app.35578
Published online 28 December 2011 in Wiley Online Library (wileyonlinelibrary.com).

ABSTRACT: Control possibility of the electrospinning process appears to be one of the most challenging tasks in the manufacturing of fibrous structures. At the same time, its versatility and simplicity make electrospinning one of the most popular nanotechnology method for the production of one-dimensional nanostructures. In this study, focused electrospinning of nylon, polylactic acid-copoly-caprolactone (PLACL), and poly(vinyl chloride) (PVC) fibers is thoughtfully studied. It has been found that electric field modification by electrostatic lenses, capillary-nozzle tip-to-collector electrode distance, and polymer-solvent composition are the critical parameters to achieve small deposition spots with good fibers quality. Upon optimization, nylon, PLACL, and PVC fibers deposition to fabricate a confined area with less than 4 mm, diameter and fibers stripes with a width of 0.15 mm are achieved. © 2011 Wiley Periodicals, Inc. J Appl Polym Sci 125: 820–827, 2012

Key words: fibers; membranes; structure–property relations; electrostatic field effect

INTRODUCTION

Electrospinning is a process for the fabrication of polymer fibers with diameters in a micro and nanometer range by using an electrostatic field.[1–3] Patented in 1902 by Cooley,[4] it was rediscovered for research in the 1990s.[3,5] Currently, it is the only method for the fabrication of continuous fibers at nanometer range.[3,6] Electrospun fibers membranes have found numerous applications in bioengineering, microelectronics, energy technology, and environmental engineering.[3,6–17]

Complex electrohydrodynamic processes involved in conventional electrospinning cause bending instability of the electrospun jet[1,18] resulting in spots with a diameter exceeding 100 mm, usually covering the whole collector. The fibers spots often do not show sharply defined boundaries. Large deposition spot limits strongly potential application fields where high precision of the deposition is required as well as it causes significant wastage of the electrospun material. During the last years, efforts have been done to make electrospinning more controllable. Kim et al.[19] applied cylindrical auxiliary electrodes above the capillary-nozzle to achieve a stable electrospinning of polycaprolactone (PCL) microfibers. The obtained microfiber spot diameter was 22 mm. By introducing positively charged series of ring electrodes between the capillary-nozzle tip and the collector, Deitzel et al.[20] electrospun polyethylene oxide 300 nm diameter fibers with water-based solution and achieved a fibers spot diameter of 10 mm.

In this study, we have added simple and effective electrostatic lens systems to the classic electrospinning setup to minimize the diameter of controllable fibers deposition spot. The developed approach has been evaluated with electrospinning of biocompatible PLACL as well as nonbiocompatible Nylon and poly(vinyl chloride) (PVC). The influence of the different configurations of electrostatic lens systems, the distance between the capillary-nozzle tip, and the collector electrode as well as the collector size on controlling the fibers deposition spot size was also studied. To achieve a more profound understanding for the impact of these parameters, experiments and numerical modelling were taken into account. Under optimized conditions, the fibers spot diameter of below 4 mm was achieved while maintaining the uniformity and good quality of the fibers. With continuous movement of the collector, fibers stripes of 0.15 mm width were fabricated.

Correspondence to: D. Pliszka (nnidp@nus.edu.sg).
Contract grant sponsor: A*STAR, Singapore (project 'Fabrication of Novel Nanocomposite Filter Membranes for Understanding Basic Principles and Their Advanced Technology Applications); contract grant number: R-398-000-041-305.
Contract grant sponsor: NRF-Technion; contract grant number: R-398-001-065-592.

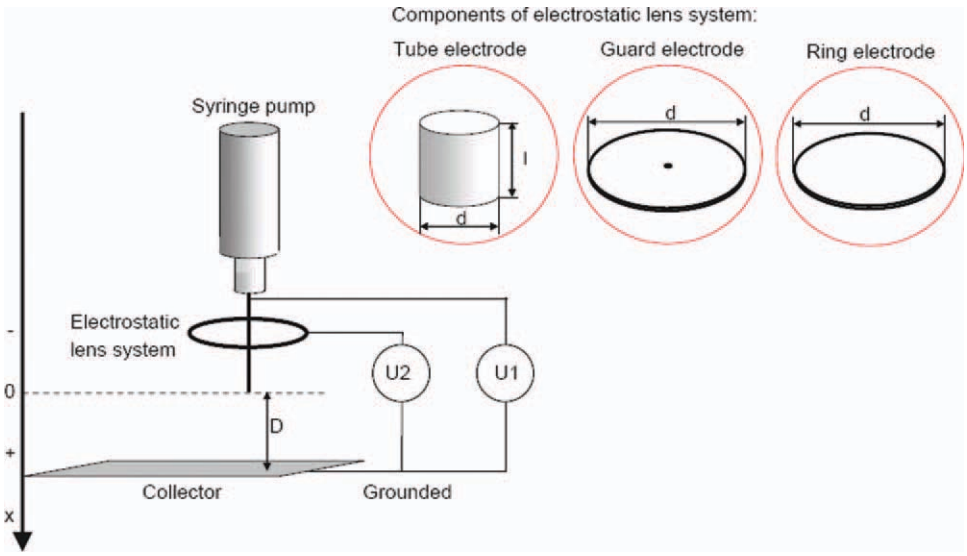

Figure 1 Setup for electrospinning of polymer fibers with electrostatic lens system. [Color figure can be viewed in the online issue, which is available at wileyonlinelibrary.com.]

EXPERIMENTAL

Materials

For this study, the polymers PVC (M_w 233,000 Da; Sigma-Aldrich, USA), Nylon-6 (UBE, Japan), and poly(L-lactic acid)-*co*-poly-(3-caprolactone) (PLACL) (70 : 30, M_w 150,000 Da; Boehringer Ingelheim Pharma GmbH & Co., Germany) were used.

They were dissolved in *N*,*N*-dimethylformamide (DMF; ACS reagent = 99.8%; Sigma-Aldrich, Germany), tetrahydrofuran (THF; purity = 99.0%; Merck, Germany), dichloromethane (DCM; purity = 99.8%; Merck, Germany), and 1,1,1,3,3,3-hexafluor-2-propanol (HFP; purity = 99%; Sigma-Aldrich, Germany) without any further purification.

Electrospinning

Nylon solution A and B: Nylon was dissolved in HFP at a concentration of 10% (w/v) for Nylon solution A and 26% (w/v) for Nylon solution B.

PLACL solution A and B: PLACL was dissolved in HFP at a concentration of 10% (w/v) for PLACL solution A and 26% (w/v) for PLACL solution B.

PVC solution A: PVC was dissolved at a concentration of 10% (w/v) in DMF and THF used in equal amounts.

PVC solution B: 0.3 g of PVC was added to DCM, DMF, and THF used in equal amounts (1 mL) and steered for 2 h at 35°C. After another 24 h of stirring at 20°C, 1.5 mL of THF was added. The solution was stirred for another 24 h.

If not differently stated, the solutions were stirred for 24 h and electrospun with the modified setup (Fig. 1). GAMMA High Voltage Research (USA) and Glassman High Voltage (USA) power supplies were used.

Electrospinning was performed using modified electrospinning setup with additional electrostatic lenses. Details of the electrodes arrangements are given within the text. To provide better understanding of the electrodes positions, we introduced the coordinate axis x in vertical direction with the capillary-nozzle tip as zero point ($x = 0$ mm) with positive values toward the collector and negative ones above the capillary-nozzle tip. The position of the electrodes was measured from their bottom edge. The length was only a relevant parameter for the tube electrode. The distance between the capillary-nozzle tip and the collector was defined as D. All dimensions were given in mm (Fig. 1).

The following electrospinning parameters were defined by the setup: where D is the distance between the capillary-nozzle tip and the collector, $U1$ the voltage applied to capillary-nozzle tip, $U2$ the voltage applied to electrostatic lens system, x the position of the components of the electrostatic lens system, d the diameter of the components of the electrostatic lens system, and l the height of the components of the electrostatic lens system.

Characterization

Fibers morphology and fibers membrane quality were examined by scanning electron microscope (SEM) QUANTA 200F from FEI (Netherlands) preceded by gold sputtering (JEOL JFC-1600, Auto Fine Coater, Japan).

The pore size distribution was determined from bubble point measurements using a capillary flow porometer (Porous Materials, USA) by complete wetting of the membranes with Galwick (Porous Materials).[21]

TABLE I
Impact of Ring Electrode Position with $d = 33$ mm on the Fibers Spot Size and Fibers Diameter

Polymer solution	Electrode position (mm)	Voltage V1 and V2 (kV)	Flow rate (mL/h)	Spot size (mm)	Fibers diameter (nm)
Nylon A	–	14	1.0	Not defined	357 ± 62
	−15	14	1.0	59.6 ± 3.5	495 ± 88
	0	21	1.0	33.5 ± 1.9	1141 ± 293
PLACL A	–	14	1.0	Not defined	602 ± 106
	−15	14	1.0	59.6 ± 3.4	631 ± 135
	0	21	1.0	31.3 ± 2.1	1351 ± 174
PVC A	–	10	1.0	Not defined	607 ± 127
	−15	10	1.0	69.5 ± 2.1	632 ± 96
	0	17	1.0	32.5 ± 1.2	765 ± 153

RESULTS AND DISCUSSION

Electrospinning, though it is a simple process, is challenging to control. Polymeric solution ejected from the capillary-nozzle tip at adjusted flow rate is subjected to electric field between supply needle and grounded collector both charged by high voltage power. Electric field between the capillary-nozzle tip and the collector causes protruding of a polymer solution droplet and deformation due to electrostatic forces. It causes transformation of hemispherical droplet to conical shape, called as Taylor cone. Upon reaching the critical voltage in the droplet, accumulated charge on the surface overcomes surface tension and an elongated continuous fiber is protruded toward the collector, and the electric field accelerates the stream onto the grounded deposition target.[22] As fiber is travelling to the grounded target solvent evaporates and with properly adjusted voltage and distance, fibers reaching collector are dry. After the fiber has been ejected from the capillary-nozzle tip, its motion is mainly determined by electrostatic forces created by the strong external electric field and surface charge collected on the electrospun fibers. In addition, the charges carried by the fibers induce opposite charges on the surface of the collecting electrode, which also help to attract the fibers to the electrode. Fluid dynamics of the charged electrospinning jet is a complex process, and the electrospinning jet will in most of the cases enter a "whipping mode."[18] Origin of this chaotic motion is in a complicated interaction of factors that include solution viscosity, surface tension, solvent evaporation rate, conductivity of the electrospun polymeric solution, electrostatic forces, air friction, and gravity.[18,23] It is a main mechanism of the achieving nanometers range of fibers diameters—during the whipping movement of the fibers jet, not fully dried fibers are elongating and its diameter is decreasing due to acting forces. Longer exposition photographs reveal the electrospinning jet envelope cone. It was a clear direction for this study that reduction of the deposition spot could be achieved by the elongation of the stable electrospinning jet part and suppression of the envelope cone diameter.

In our study, we performed a systematic analysis of the influence of the various electrostatic lenses as well as other parameters like distance between capillary-nozzle tip and the collector in the system with electrostatic lenses applied and also polymeric solution composition. Besides, the simplicity of the system was an important factor for us to make the technology available to a wider researcher community and potential commercialization.

Single ring electrode

An electrostatic lens system consisting of one ring electrode with $d = 33$ mm charged with the same potential as the capillary-nozzle tip was added to the electrospinning setup (Fig. 1) for Nylon, PLACL, and PVC fibers fabrication with the electrospinning conditions as in Table I. D was maintained at 120 mm.

Often experienced instability of the electrospinning at the nozzle-tip is caused by partial drying of the polymer solution or imperfections in flat face preparation of the nozzle-tip leads. Using additional ring electrode greatly eliminated this instability. The length of the stable straight jet was elongated due to suppression of the bending instability onset by the electrostatic field modified by the additional ring electrode. As a result, electrospinning cone was smaller, and therefore smaller fibers spot size was achieved (see Table I). With a ring electrode placed above the capillary-nozzle tip ($x = -15$ mm), a defined spot size with a diameter between 60 and 70 mm was achieved for all electrospun polymers. Shifting the ring electrode toward the capillary-nozzle tip, the spot size could be decreased to a defined size of about 30 mm diameter. Simultaneously, the voltage was increased by 7 kV in order to maintain stable electrospinning. The spot size slightly varied due to the polymer different molecular weight and properties of the electrospun polymers and due to the different solution properties.

The decrease of the spot size had an impact on the average fibers diameter (Table I). With enhanced focusing effect, bending instability of the polymer jet

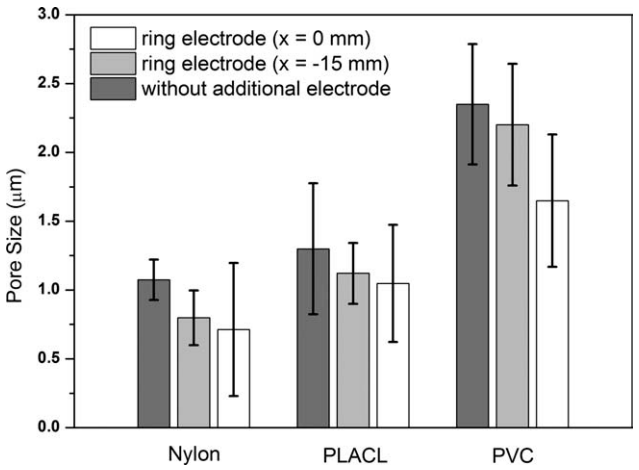

Figure 2 Pore sizes without any additional electrode, with additional ring electrode ($x = -15$ mm) and with additional ring electrode ($x = 0$ mm) for Nylon, PLACL, and PVC.

was reduced, and therefore polymer jet stretching due to its movement was suppressed. The degree of this effect varied depending on the polymer and the polymer solution property. Not only was the average diameter increased by shifting the metal ring toward the needle tip, but the fibers diameter uniformity also increased due to less stable electric field in terms of spatial distribution.

For all tested polymers, the pore size was reduced by applying an additional ring electrode ($x = -15$ mm). The trend of reducing the pore size was enhanced by shifting the additional ring electrode toward the capillary-nozzle tip ($x = 0$ mm) and by increasing the voltage by 7 kV (Fig. 2) effecting in reduction of deposition spot area. The development of the pore size could be mainly correlated to the collected fibers spot size as a result of higher density of the fibers collected per area for smaller deposition spots, because the same amount of the material is collected on much smaller area. This effect overlaps increase of the pore sizes caused by the larger fibers diameters with decreased spot size (see Table I).

As shown earlier, all polymers showed similar behavior with the additional ring electrode. Therefore, PVC solution A was chosen for further optimization.

Guard electrode

A guard electrode was a metal disc fixed co-axially at the nozzle and charged with the same potential. Similarly, like in ring electrode, the electrospinning cone axis was more stable, the electrospinning cone angle was narrower due to a more homogeneous electrostatic field distribution, the length of the straight jet in the electrospinning process was increased, and the system could be operated in a wider voltage range.

Guard electrodes of various diameters were applied at different positions (Table II). Large guard electrodes with $d = 100$ mm suppressed the electrospinning process at any position. The electrostatic field between the needle tip and the collector was too weak to initiate releasing of any fiber. For a smaller guard, electrode with $d = 50$ mm and positioned at $x = -15$ mm electrospinning was not interrupted, and the fibers spot diameter was 30 mm. The fibers spot diameter could be decreased further to 25 mm by positioning the guard electrode closer to the capillary-nozzle tip at $x = -5$ mm. Because of the weakened electrostatic field between the capillary-nozzle tip and the collector, stretching the jet could not be maintained, and therefore electrospinning was interrupted. This effect did not occur for a guard electrodes with $d = 20$ mm. Fibers were produced at any guard electrode position; however, the fibers spot diameter was comparatively large with 35 mm at the minimum. Therefore, there was a compromise between the focusing effect of guard electrodes and the weakening of the electrostatic field resulting in unstable fiber formation.

The quality of the fibers produced in the system with guard electrodes was not significantly affected by the variation of the guard electrode position.

Combined ring a tube electrodes

Several combinations of the electrostatic lens system were studied. In setup 1 and 2, investigating the impact of the tube diameter, a reduction of the tube electrode diameter from $d = 11$ mm to $d = 3$ mm decreased the fibers spot diameter for $\sim 17\%$ and therefore enhanced the focusing effect (see Table III).

Tube electrodes with smaller diameter increased the average fiber diameter. The average fiber diameter was 660 ± 298 nm for a tube electrode with $d = 3$ mm and $l = 20$ mm and positioned at $x = -1$ mm. Fibers fabricated with a tube electrode with $d = 11$ mm and the other parameters remaining the same had a diameter of 521 ± 211 nm. Fibers fabricated with a small tube diameter showed significant diameter variation, but did not show any other defects.

To improve the controllability of the electrostatic field and therefore the electrospinning process, a

TABLE II
Impact of Varying Position of the Guard Electrode on the Spot Size and the Nanofiber Quality

Electrode diam. (mm)	Position x (mm)	Voltage $V1$ and $V2$ (kV)	Spot size (mm)
50	−15	10	36.4 ± 1.6
50	−5	10	23.9 ± 0.9
20	−5	10	31.4 ± 2.0

PVC solution A was electrospun with a flow rate 1.0 mL/h.

TABLE III
Correlation Between the Elements of the Electrostatic Lens System, Their Combination, the Applied Voltages U1 and U2 and the Nanofibers Spot Diameter

Setup	Electrode	Diameter d (mm)	Length l (mm)	Position x (mm)	Voltage $V1$ (kV)	Voltage $V2$ (kV)	Spot size (mm)
1	Tube	3	20	−1	12.0	12.0	34.7 ± 1.6
2	Tube	11	20	−1	12.0	12.0	42.8 ± 2.5
3	Tube	11	20	−1	11.0	7.0	20.9 ± 1.6
	Ring	20	–	8			
4	Ring 1	25	–	−1	10.0	7.8	13.4 ± 1.8
	Ring 2	30	–	16			

For all configurations, PVC solution A, a flow rate 1.0 mL/h and $D = 100$ mm were applied.

different voltage was applied to the components of the electrostatic lens system. One electrode was positioned above the capillary-nozzle tip, the other one below. A voltage of 1–2 kV lower than the voltage between the capillary-nozzle tip and the collector was applied to the electrostatic lens system to avoid the interruption of electrospinning. The effectiveness of electrostatic lens setup 3 and 4 considering focusing was investigated (see Table III). Setup 4 with two ring electrodes was found to reduce the fibers spot diameter more efficiently than the tube-ring combination (Setup 1–3). By setting ring electrode 1 at $x = 16$ mm, the length of the straight jet was increased and could therefore pass through ring electrode 2 positioned under the capillary-nozzle tip ($x = -1$ mm). The voltage applied at the electrostatic lens system 8.4 kV had to be set incrementally increased in order to maintain electrospinning. Applying the two-ring electrodes combination, the fibers spot diameter was reduced by over 40% in comparison with tube-ring electrode combination to 12 mm (Table III). However, the fibers quality was unsatisfactory for the two-ring electrodes combination because of fused fibers due to the insufficient solvent evaporation. Insufficient solvent evaporation was explained with the smaller electrospinning cone size and therefore the shorter flight time of the fiber from the capillary-nozzle tip to the collector. Furthermore, the average fiber diameter was larger than 1 μm.

Collector size and distance

By reducing the collector size and replacing the aluminium square collector with an edge length of 150 mm by a aluminium stripes with 16 mm and 6 mm width as well as by a 0.1-mm copper wire, the fibers spots had the shape of an ellipsis with a minor axis of 10 mm at the minimum and an undefined major axis size. With decreasing collector size, a weakened electrostatic field between the capillary-nozzle tip and the collector was observed. Because of the weak electrostatic field between the capillary-nozzle tip and the collector, no combination of a small collector and electrostatic lens systems could be achieved. Therefore, the focus was shifted from studying the impact of reduced collector size to the effect of a smaller D.

Halving D from 100 to 50 mm and applying a tube electrode as the electrostatic lens system (Table IV), the fibers spot diameter was decreased by 25% from 30 to 22 mm for optimized electrospinning conditions. However, for smaller D, the average fiber diameter increased from 511 ± 211 nm (for $D = 100$ mm) to 547 ± 177 nm ($D = 50$ mm) and the fiber deposition was less uniform. These negative effects of smaller D were explained with the shorter way to stretch the fibers in the electrostatic field. These results support earlier observations.[24]

The application of an electrostatic lens system consisting of two ring electrodes resulted in a stronger focusing effect (Table IV). The fibers spot diameter was reduced from 12 to 6 mm with $D = 116$ and $D = 66$ mm, respectively. Because of the reduced travel distance of the fibers between the capillary-nozzle tip and the collector, the fibers were fused together after their deposition on the collector. In addition, the fiber diameter increased significantly with decreasing D. To

TABLE IV
Impact of the Distance D Between the Capillary-Nozzle Tip and the Collector on the Nanofibers Spot Size

D (mm)	Electrode	Diameter d (mm)	Length l (mm)	Position x (mm)	Voltage $U1$ (kV)	Voltage $U2$ (kV)	Spot size (mm)
100	Tube	11	20	−1	12.0	12.0	42.8 ± 2.5
50	Tube	11	20	−1	12.0	12.0	25.5 ± 1.4
116	Ring 1	25	–	−1	10.0	7.7	13.4 ± 1.8
	Ring 2	30		16			
66	Ring 1	25	–	−1	10.0	7.7	4.55 ± 0.38
	Ring 2	30		16			

For all configurations, PVC composition A and a flow rate 1.0 mL/h were applied.

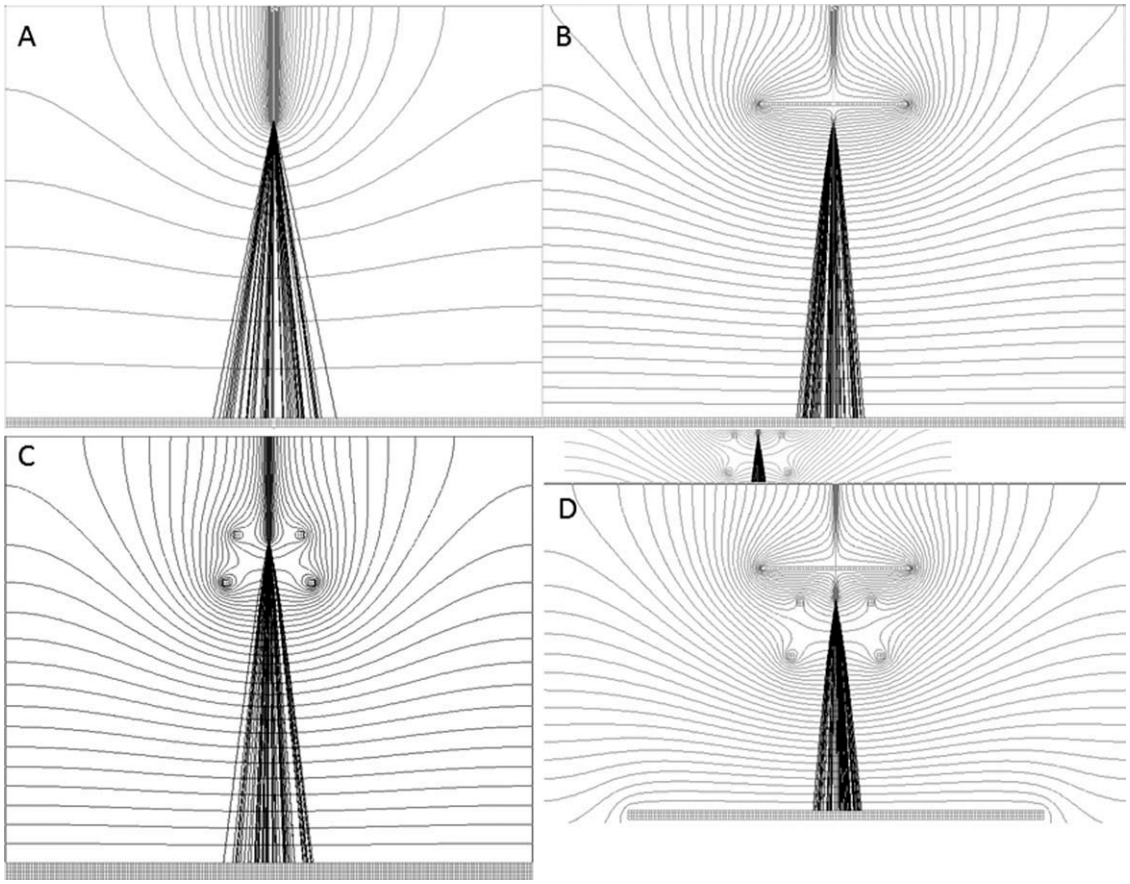

Figure 3 SIMION 8.0 modeling of potentials for (A) classics electrospinning setup (10 kV), (B) guard electrode (20 mm diameter) 5 mm above spinneret tip (10 kV), (C) two ring electrodes (25 and 30 mm diameters): 1 mm above spinneret tip and 16 mm below spinneret (spinneret: 10 kV, electrodes 7.7 kV), (D) optimized electrodes setup (note smaller distance from the collector).

facilitate solvent evaporation from the electrospun fibers, a hot air draft was introduced into the setup perpendicular to the collector and at a 45° angle.

Numerical modeling

The experimental conditions were tested by modeling electric field distribution using SIMION Version 8.0 (Scientific Instrument Services, USA)—usually used for ion beam trajectories modeling in electron optics devices, but also has been found useful for our purpose. The software used has a possibility to create 3D models of the electrodes setups used in the experiments. Because its main application is beam trajectories modeling, simulation results are given as equipotential lines of the electric field, acting as electrostatic lenses for any charged particles being passed through the modelled system. Flexibility and ease of preparation of different designs is a big advantage of the SIMION. It could be instantly checked how different electrospinning parameters, especially voltage applied were acting on the ions beam. One can note that ion beam may be considered far from electrospinning jet, but modeling results shown great accordance with observed experimental results; therefore, this method allowed us to avoid spending much time on testing all possible arrangements experimentally. Only a selection of modelling results has been shown in the work (Fig. 3). Classic electrospinning [Fig. 3(A)] shows the most wide spot size and less uniform electric field distribution. Modified setups with guard electrode [Fig. 3(B)] and two ring electrodes [Fig. 3(C)] give more uniform electric field distribution and decreased modeled collection spot size. Optimized setup described in detail in the next paragraph is a combination of guard electrode and two ring electrodes and gives the smallest achieved spot size [Fig. 3(D)].

Optimized setup

As shown earlier, one of the two most effective methods to reduce the fibers spot size was the reduction of D, the fibers fusion had to be prevented. Two approaches were studied: the amount of solvent had to be reduced (polymer concentration increased), and solvents were substituted by ones with lower vapour pressure (faster evaporation).

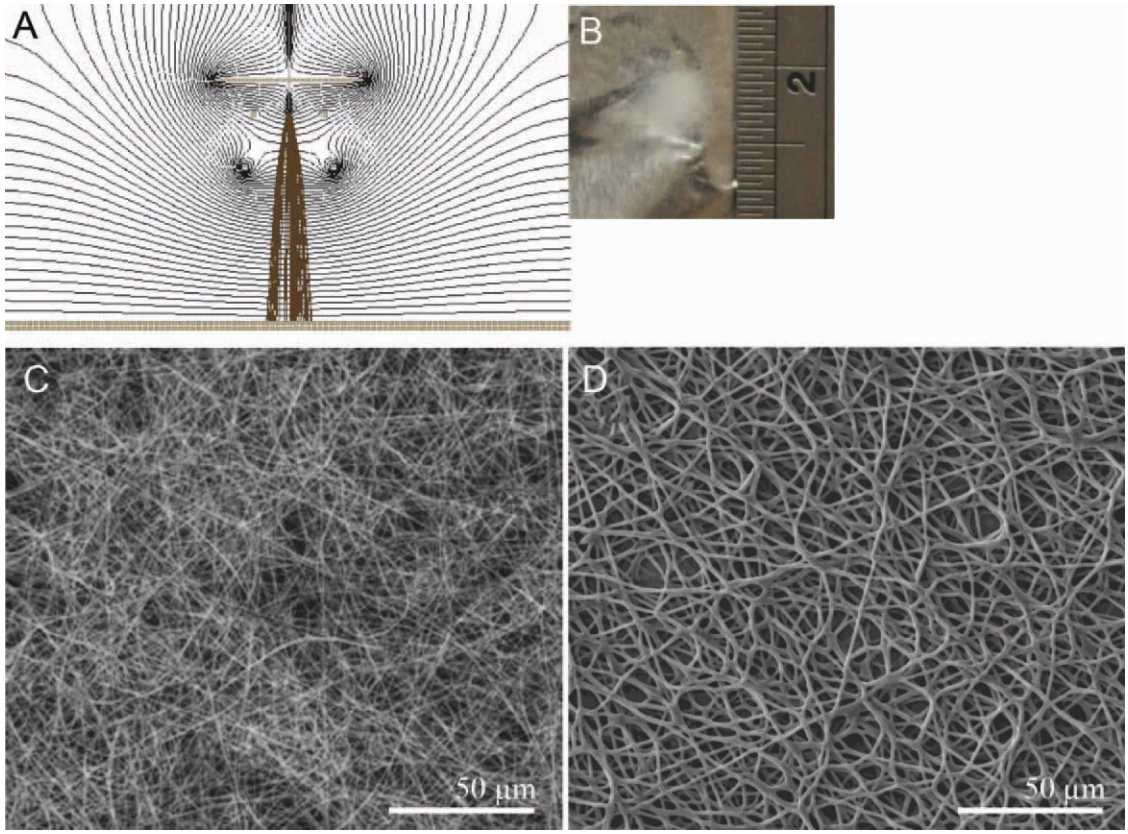

Figure 4 Fibers electrospun under optimized conditions (Table V) with flow rate 1.0 mL/h and $D = 70$ mm on a static collector. Components of the electrostatic lens system: guard electrode with $d = 50$ mm positioned at $x = -10$ mm, ring electrode 1 with $d = 25$ mm positioned at $x = 1$ mm and ring electrode 2 with $d = 30$ mm and positioned at $x = 17$ mm. A: Morphology of PVC solution B and (B) morphology of Nylon fibers. On the inset photography of the PVC fibers spot. [Color figure can be viewed in the online issue, which is available at wileyonlinelibrary.com.]

For PVC, the electrospinning setup accomplished with an electrostatic lens system was optimized consisting of a guard electrode with $d = 50$ mm positioned at $x = -10$ mm combined with two ring electrodes with the dimension $d = 25$ mm positioned at $x = 1$ mm and $d = 30$ mm positioned at $x = 17$ mm. Distance between the capillary-nozzle tip and the collector was $D = 70$ mm, and the flow rate of the electrospinning solutions was 1 mL/h (Fig. 4).

PVC solution B with faster evaporating solvents was applied. THF and DMF, DCM were used as solvents due to its high vapor pressure of 46,700 Pa in comparison with a vapour pressure of 347 and 17,200 Pa for DMF and THF, respectively. Resulting electrospinning spot size was 3.74 ± 0.37 mm [Fig. 4(B), Table V], and thin fibers with a diameter 193 ± 40 nm [Fig. 4(C), Table V] were obtained.

The optimized setup was tested with both remaining polymers: Nylon and PLACL. The polymer solutions were adapted by increasing the polymer concentration to 26% (w/v) (Nylon solution B and PLACL solution B). The spot size was reduced to 3–4 mm diameter; however, due to the high polymer concentration and therefore low solution viscosity, the fibers diameter exceeded 1000 nm in both cases (Table V).

Comparison of the achieved spot size with similar approaches shows its advantage. Using cylindrical electrodes above, the capillary-nozzle spinneret by Kim et al.[19] resulted in electrospinning spot diameter of 22 mm. More complex approach of Deitzel et al.[20] with series of concentric electrodes in area between the spinneret and the collector gave a spot size of 10 mm diameter. In our approach, we were able to achieve much smaller spot. It is worthwhile to mention work of Bellan et al.[25] who achieved a fibers spot diameter of 5 mm for PCL fibers. In contrary to our approach, to focus electrospinning, a complex

TABLE V
Nylon, PLACL, and PVC Fibers Were Electrospun with $D = 70$ mm and a Flow Rate 1.0 mL/h

Polymer solution	Voltage $V1$ (kV)	Voltage $V2$ (kV)	Spot size (mm)	Fiber diameter (nm)
Nylon B	14.0	9.5	3.65 ± 0.58	1201 ± 250
PLACL B	14.0	9.5	3.71 ± 0.47	1790 ± 422
PVC B	12.8	10.2	3.74 ± 0.37	193 ± 40

Components of the electrostatic lens system: guard electrode with $d = 50$ mm positioned at $x = -10$ mm, ring electrode 1 with $d = 25$ mm positioned at $x = 1$ mm and ring electrode 2 with $d = 30$ mm and positioned at $x = 17$ mm.

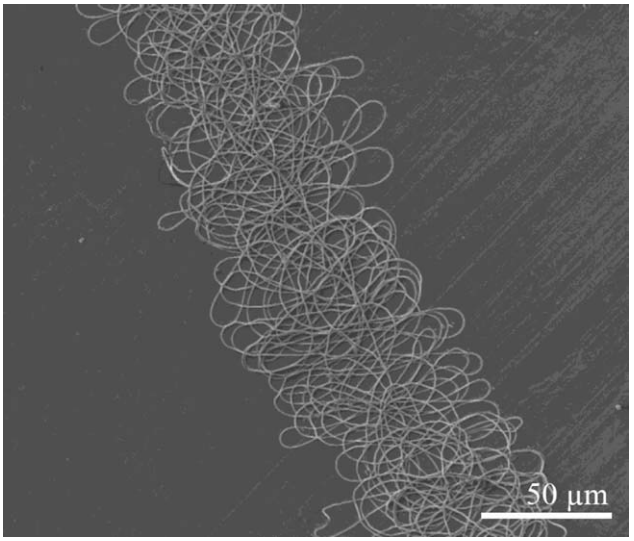

Figure 5 PLACL fibers electrospun under optimized conditions (Table V) with a flow rate 1.0 mL/h and D = 70 mm on a collector moving with $\sim$ 0.1 m/s. Components of the electrostatic lens system: guard electrode with d = 50 mm positioned at $x = -10$ mm, ring electrode 1 with d = 25 mm positioned at x = 1 mm and ring electrode 2 with d = 30 mm and positioned at x = 17 mm. The fibers line had a width of 0.158 ± 0.013 mm.

four-electrode setup controlled with computer-controlled switchable power supplies was positioned between the capillary-nozzle tip and collector.

An interesting result is a collection of the nanofibers on the moving collector. It was tested due to the fact long deposition time (about one minute) of the fibers on a single spot caused a creation of solid button-like structure due to high solvent concentration and redissolving of the fibers. With a collector moving with a speed of $\sim$ 0.1 m/s, fibers lines with a width 0.158 ± 0.013 mm were electrospun (Fig. 5). Because of the stretching of the polymer due to the collector movement, the fiber diameters were reduced to 833.1 ± 115.6 nm and 1177.8 ± 122.7 nm for Nylon and PLACL, respectively. These lines were a promising tool for the precise deposition of fibers and the fabrication of fine structures. It may suggest that actual deposition spot size is smaller than 4 mm, but collection of the charged fibers and their repulsive interaction with incoming fibers caused increase of the spot diameter to measured 4 mm.

CONCLUSIONS

In this work, simple electrostatic lens systems were shown as an useful tool to control deposition spot of the electrospun fibers. Focusing effect was shown for a variety of different polymers and solvents. Optimization of the setup procedure gave a good understanding of influence of different kind of electrodes on behavior of the electrospinning jet of the fibers. Finally, an optimized electrospinning setup was designed. Spot sizes ranging 3–4 mm and fibers lines with a 0.1–0.2 mm width of good quality fibers were achieved. The membrane pore size was controlled by the voltage as well as the ring electrode position: increasing voltage and distance between the ring electrode and capillary-needle tip resulted in diminished pore size. This correlation is of highest importance for the fabrication of filter membranes in order to determine a defined filter performance and for tissue engineering scaffolds to achieve cell differentiation. Our goal was to create a simple method to control deposition spot size and this target was achieved with success. The presented results are the first step for further increase of the electrospinning controllability for its application in fabrication of microelectronic devices as well in bioengineering, where highest possible level of control is required.

References

1. Reneker, D. H.; Chun, I. Nanotechnology 1996, 7, 216.
2. Pawlowski, K. J.; Belvin, H. L.; Raney, D. L.; Su, J.; Harrison, J. S.; Siochi, E. J. Polymer 2003, 44, 1309.
3. Li, D.; Xia, Y. N. Adv Mater 2004, 16, 1151.
4. Cooley, J. F. US Pat. No.692,631 (1902).
5. Doshi, J.; Reneker, D. H. J Electrost 1995, 35, 151.
6. Greiner, A.; Wendorff, J. H. Angew Chem Int Ed 2007, 46, 5670.
7. Sundarrajan, S.; Ramakrishna, S. J Mater Sci 2007, 42, 8400.
8. Huang, Z. M.; Zhang, Y. Z.; Kotaki, M.; Ramakrishna, S. Compos Sci Technol 2003, 63, 2223.
9. Subbiah, T.; Bhat, G. S.; Tock, R. W.; Pararneswaran, S.; Ramkumar, S. S. J Appl Polym Sci 2005, 96, 557.
10. Ramaseshan, R.; Sundarrajan, S.; Liu, Y. J.; Barhate, R. S.; Lala, N. L.; Ramakrishna, S. Nanotechnology 2006, 17, 2947.
11. Choi, S. S.; Lee, S. G.; Im, S. S.; Kim, S. H.; Joo, Y. L. J Mater Sci Lett 2003, 22, 891.
12. Choi, S. S.; Lee, S. G.; Joo, C. W.; Im, S. S.; Kim, S. H. J Mater Sci 2004, 39, 1511.
13. Barhate, R. S.; Sundarrajan, S.; Pliszka, D.; Ramakrishna, S. Filtr Sep 2008, 45, 32.
14. Roso, M.; Sundarrajan, S.; Pliszka, D.; Ramakrishna, S.; Modesti, M. Nanotechnology 2008, 19, 6.
15. Lala, N. L.; Thavasi, V.; Ramakrishna, S. Sensors 2009, 9, 86.
16. Thavasi, V.; Renugopalakrishnan, V.; Jose, R.; Ramakrishna, S. Mater Sci Eng R-Rep 2009, 63, 81.
17. Thavasi, V.; Singh, G.; Ramakrishna, S. Energy Environ Sci 2008, 1, 205.
18. Reneker, D. H.; Yarin, A. L.; Fong, H.; Koombhongse, S. J Appl Phys 2000, 87, 4531.
19. Kim, G. H.; Han, H.; Park, J. H.; Kim, W. D. Polym Eng Sci 2007, 47, 707.
20. Deitzel, J. M.; Kleinmeyer, J. D.; Hirvonen, J. K.; Tan, N. C. B. Polymer 2001, 42, 8163.
21. Porter, M. C. Handbook of Industial Membrane Technology; Noyes: Park Ridge, NJ, 1990.
22. Yarin, A. L.; Koombhongse, S.; Reneker, D. H. J Appl Phys 2001, 89, 3018.
23. Shin, M. K.; Kim, S. I.; Kim, S. J. Appl Phys Lett 2006,88.
24. Ramakrishna, S.; Fujihara, K.; Teo, W. E.; Lim, T. C.; Ma, Z. An Introduction to Electrospinning and Nanofibers; World Scientific: Singapore, 2005.
25. Bellan, L. M.; Craighead, H. G. J Vac Sci Technol 2006, B24, 3179.